J. Plasma Physics (1998), *vol.* 60, *part* 4, *pp.* 845–859. Printed in the United Kingdom
© 1998 Cambridge University Press

Solitons in multi-ion plasmas

PETER HACKENBERG,[1] GOTTFRIED MANN[1]
and ECKART MARSCH[2]

[1] Astrophysikalisches Institut Potsdam,
An der Sternwarte 16, D-14482 Potsdam, Germany

[2] Max-Planck-Institut für Aeronomie,
Postfach 20, D-37191 Katlenburg-Lindau, Germany

(Received 30 March 1998)

In the heliosphere large fluctuations of the magnetic field are sometimes observed, especially at shocks (e.g. travelling interplanetary shocks, planetary bow waves, and shocks related to corotating interaction regions). The large fluctuations very often have an amplitude that reaches easily four or five times the magnitude of the quiet magnetic field. Since the plasma mostly contains a non-negligible fraction of heavy ions (e.g. helium ions or cometary water ions), these magnetic field fluctuations are described in terms of three-fluid equations. Here electrons, protons and heavy ions are considered as separate fluids interacting with themselves by electromagnetic forces. The three-fluid equations are treated in such a way that we are searching for one-dimensional stationary waves. Thus the equations are reduced to a fully nonlinear set of ordinary differential equations, which have been evaluated numerically with respect to solitary waves. Subsequently, examples of solitary waves in a electron–proton plasma loaded with 10 % $^4He^{2+}$ ions are presented. For instance, an enrichment of helium ions is observed within the solitary waves.

1. Introduction

Large-amplitude magnetic field fluctuations at low frequencies are often observed by in situ measurements at discontinuities in the solar wind. Such discontinuities are, for instance, the Earth's bow shock (see e.g. Paschmann *et al.* 1979; Hoppe *et al.* 1981; Mann and Lühr 1991), other planetary shocks (see e.g. Fairfield and Behannon 1976; Goldstein *et al.* 1983), cometary shocks (see e.g. Tsurutani 1991), and corotating interaction regions (CIRs) of the solar wind (see e.g. Tsurutani *et al.* 1995). It should be noted that the plasma in these regions usually shows a non-negligible abundance of more-or-less heavy ions, which originate from the planetary atmospheres (e.g. oxygen ions) or the cometary nucleus (water group ions) or which are just an ordinary component of the solar wind (helium ions; see e.g. Marsch *et al.* 1982).

Another phenomenon is that of so-called *magnetic holes* (Turner *et al.* 1977), which are 'isolated intervals when the magnitude of the interplanetary magnetic field drops to a few tenths, or less, of its ambient value for a time that corresponds to a linear dimension of tens to a few hundreds of proton gyro-radii' (Winterhalter *et al.* 1994). Recently, Baumgärtel *et al.* (1997) have suggested solitons as a possible explanation of these holes.

https://doi.org/10.1017/S0022377898007193 Published online by Cambridge University Press

We do not intend here to explain the above-mentioned phenomena. But they have motivated us, to study nonlinear waves in multi-ion plasmas.

To the best of our knowledge, there have been few theoretical investigations on this topic. Apart from particle simulations, multi-ion plasmas have usually been treated in the linear approximation (see e.g. Oscarson and André 1986; McKenzie *et al.* 1993; Miller and Viñas 1993; Thompson *et al.* 1995; Gnavi *et al.* 1996; Mann *et al.* 1997), or some rather special assumptions are made: Isenberg and Hollweg (1982) assumed for example that there are no particle density fluctuations. Verheest (1990) only investigated circularly polarized Alfvén waves propagating parallel to the ambient magnetic field.

Therefore we think it is very promising to undertake some investigations on nonlinear multi-ion plasmas. Since there are a great variety of ways in which this can be done, we consider a homogeneous, magnetized and collisionless three-component plasma consisting of electrons, protons and ions. Furthermore, we assume that the fluctuations are propagating only in one dimension (parallel to the x axis), and that the fluctuations become stationary in a comoving frame of reference.

We describe the plasma using multifluid equations. Since the frequency scale of the above-mentioned fluctuations is very much smaller than the plasma frequency and the electron cyclotron frequency Ω_e, and is mostly even smaller than the proton cyclotron frequency Ω_p, these fluctuations are predominantly carried by the motions of the ions, and the electrons merely act as a neutralizing fluid. This allows us to simplify the multifluid equations, by assuming quasineutrality and neglecting the displacement current and the electron mass. Thus we end up with a set of ordinary differential equations (ODEs) of order six.

Since the amplitude of the observed fluctuations may be large (sometimes up to a few times the magnitude of the undisturbed magnetic field), a fully nonlinear description of the plasma is necessary, and we cannot neglect a priori any nonlinear terms. Therefore we must rely on numerical methods to solve the ODEs, which will be done in Sec. 4.

In particular, we are interested in searching for solitary-wave solutions of the stationary multifluid equations. It is well known that solitons represent a purely nonlinear phenomenon and have no analogue in linear wave theory.

Nevertheless, we start (see Sec. 3) our investigation with a linearized set of equations, and apply it to the small-amplitude tails of the solitary wave. Thus two goals are achieved: first, we obtain a necessary condition for the existence of the solitary waves, and, secondly, we get appropriate initial values for the numerical integration of the nonlinear ODEs.

2. Basic equations

We shall describe the magnetized and collisionless plasma by means of multifluid equations, which can be derived from the Vlasov equation (Krall and Trivelpiece 1973; Mann *et al.* 1997) and are supplemented with the Maxwell equations. This set of equations is closed by a polytropic equation of state (with isotropic pressure and adiabatic index γ_α) for each particle component.

The plasma consists of three different species, namely electrons, protons and ions with the mass $m_i = Mm_p$ and charge $q_i = Ze$, which are specified relative to the proton mass m_p and the (positive) elementary charge e. The unperturbed number densities $N_{0\alpha} = \kappa_\alpha N_0$ (α is our general species index, and takes the values e, p and

https://doi.org/10.1017/S0022377898007193 Published online by Cambridge University Press

i) are given relative to some arbitrary number density N_0, which is taken to be the electron number density, i.e. $\kappa_e = 1$. If we specify the relative unperturbed ion density by $\kappa_i = \kappa$, then, owing to charge neutrality, the relative proton density is given by $\kappa_p = 1 - Z\kappa$.

Despite the fact that the typical time and length scales of the phenomena of interest may vary rather drastically within the heliosphere, e.g. $L \approx 30$ m, $T \approx 80$ μs at the solar corona and $L \approx 600$ km, $T \approx 80$ s at Jupiter (see Bird and Edenhofer 1990; Mariani and Neubauer 1990), the same set of equations is still valid. For theoretical investigations, it is convenient to render the equations independent of the actual scales by normalization of time and space. Therefore we normalize the time with the inverse of the proton cyclotron frequency $\boldsymbol{\Omega}_p = eB_0/m_pc$ (where B_0 is the magnitude of the undisturbed magnetic field and c is the velocity of light), and the spatial coordinates are given in terms of the reference length, $l_{\rm ref} = [m_pc^2/(4\pi N_{0e}e^2)]^{1/2}$. Then the reference velocity is found to be $v_{\rm ref} = l_{\rm ref}\boldsymbol{\Omega}_p = B_0/(4\pi m_pN_{0e})^{1/2}$. The speed $v_{\rm ref}$ corresponds to the Alfvén velocity in a pure electron–proton plasma with undisturbed electron number density N_{0e}. Note that this normalization is independent of the composition of the plasma. The magnetic field $\mathbf{B}$, the particle number densities N_α and all velocities are normalized by the undisturbed background magnetic field $B_{\rm ref} = B_0$, the unperturbed particle number densities $N_{{\rm ref}\alpha} = N_{0\alpha}$ and the velocity of reference $v_{\rm ref}$ respectively. The unperturbed temperature $T_{0\alpha}$ and the unperturbed partial pressure $p_{0\alpha}$ are expressed by the plasma betas

$$\beta_\alpha = \frac{8\pi p_{0\alpha}}{B_0^2} = \frac{8\pi N_{0\alpha}k_BT_{0\alpha}}{B_0^2}\,, \tag{2.1}$$

which are already dimensionless quantities.

Since we are interested only in slow ($V_\alpha \lesssim v_{\rm ref} \ll c$) and large-scale phenomena (with typical length scales not much smaller than $l_{\rm ref}$), and the plasma is not too warm (i.e. the Debye length is very much below $l_{\rm ref}$), we are allowed to assume quasineutrality and to neglect the displacement current (see Kakutani *et al.* 1967). Furthermore, we shall neglect the electron mass with respect to the proton and other ion masses.

Supposing that the wave is propagating along the x axis, all varying quantities depend only on the time t and the x coordinate, and the normalized set of equations (from now on, all quantities are normalized, unless otherwise noted) takes the following form. The multifluid equations consist of the continuity equation

$$\frac{\partial}{\partial t}N_\alpha + \frac{\partial}{\partial x}N_\alpha V_{\alpha x} = 0 \tag{2.2}$$

and the momentum equations

$$M_\alpha\left(\frac{\partial}{\partial t}\mathbf{V}_\alpha + V_{\alpha x}\frac{\partial}{\partial x}\mathbf{V}_\alpha\right) + \frac{\beta_\alpha \mathbf{e}_x}{2\kappa_\alpha N_\alpha}\frac{\partial}{\partial x}N_\alpha^{\gamma_\alpha} - Z_\alpha\left(\mathbf{E} + \mathbf{V}_\alpha \times \mathbf{B}\right) = 0 \tag{2.3}$$

for protons ($\alpha = p$) and ions ($\alpha = i$). Owing to the neglect of the electron mass ($M_e = 0$), the electron momentum equation reduces to

$$\mathbf{E} = -\mathbf{V}_e \times \mathbf{B} - \frac{\beta_e}{2N_e}\,\mathbf{e}_x\,\frac{\partial}{\partial x}N_e^{\gamma_e}, \tag{2.4}$$

https://doi.org/10.1017/S0022377898007193 Published online by Cambridge University Press

giving an expression for the electric field. The electromagnetic fields are governed by the induction equation

$$\frac{\partial}{\partial x} E_y = -\frac{\partial}{\partial t} B_z, \qquad \frac{\partial}{\partial x} E_z = \frac{\partial}{\partial t} B_y \tag{2.5}$$

and by Ampèré's law

$$\frac{\partial}{\partial x} B_y = j_z, \qquad \frac{\partial}{\partial x} B_z = -j_y \,, \tag{2.6}$$

where the electric current is given by

$$j_y = \sum_\alpha \kappa_\alpha Z_\alpha N_\alpha V_{\alpha y}, \qquad j_z = \sum_\alpha \kappa_\alpha Z_\alpha N_\alpha V_{\alpha z} \,. \tag{2.7}$$

Owing to quasineutrality, we have been able to drop the electric charge density. By neglecting the displacement current, the x component of the electric current vanishes ($j_x = 0$). Thus the electron number density and the electron x velocity are given by

$$N_e = \kappa_p N_p + \kappa_i Z_i N_i, \tag{2.8}$$

$$V_{ex} = \frac{\kappa_p N_p V_{px} + \kappa_i Z_i N_i V_{ix}}{\kappa_p N_p + \kappa_i Z_i N_i} \tag{2.9}$$

respectively.

The x component of the magnetic field is constant ($B_x = \cos\theta$), because of $\boldsymbol{\nabla} \cdot \mathbf{B} = 0$ and the x component of the induction equation, $\partial B_x/\partial t = 0$. The variable θ is the angle between the undisturbed magnetic field and the x axis. Without further restrictions, we assume that the undisturbed, normalized, homogeneous magnetic field $\mathbf{B}_0$ is in the (x, z) plane, i.e. $\mathbf{B}_0 = \mathbf{e}_\mathrm{B} = (\cos\theta, 0, \sin\theta)$.

Now we consider a comoving frame of reference, which propagates with the velocity U and thus follows the wave. The coordinate transformation into this new system is given by

$$(x, t) \mapsto (\xi, \tau), \qquad \text{with} \quad \xi = x - Ut, \qquad \tau = t \,. \tag{2.10}$$

In particular, the substitutions

$$\left.\begin{aligned} x &\mapsto \xi + U\tau, & \frac{\partial}{\partial x} &\mapsto \frac{\partial}{\partial \xi} \\ t &\mapsto \tau, & \frac{\partial}{\partial t} &\mapsto -U\frac{\partial}{\partial \xi} + \frac{\partial}{\partial \tau} \end{aligned}\right\} \tag{2.11}$$

are to be applied to the above mentioned equations. Since we are searching for solitary waves, which are stationary in the comoving frame of reference, the τ-derivatives must vanish. Thus we obtain a system of ordinary differential equations with respect to ξ. A solitary wave is defined in such a way that all varying quantities take their unperturbed values at infinity, i.e. $\xi \to \pm\infty$. Thus integration of the continuity equation (2.2) gives

$$N_\alpha (V_{\alpha x} - U) = -U, \qquad \text{i.e.} \quad V_{\alpha x} = \frac{-U}{N_\alpha} + U \,, \tag{2.12}$$

and the induction equation (2.5) yields

$$E_y = U\,(B_z - \sin\theta), \qquad E_z = -U B_y \,. \tag{2.13}$$

https://doi.org/10.1017/S0022377898007193 Published online by Cambridge University Press

We insert the electric field just derived into (2.4), and obtain from its transverse components

$$V_{ey} = \frac{-U}{B_x}\,\frac{B_y}{N_e}, \qquad V_{ez} = \frac{-U}{B_x}\,\frac{B_z}{N_e} + \frac{U\sin\theta}{B_x} \tag{2.14}$$

the transverse electron fluid velocity. Together with (2.9), we eliminate the electron velocity from our equations. We also express the remaining longitudinal velocities $V_{\alpha x}$ in terms of the number densities N_α via (2.12).

Since the total momentum of the plasma is conserved, we are able to integrate the momentum equations (the sum over all species), and, with

$$\sum_\alpha \kappa_\alpha Z_\alpha N_\alpha \mathbf{V}_\alpha \times \mathbf{B} = \mathbf{j}\times\mathbf{B} = B_x\,\frac{\partial}{\partial\xi}\,\mathbf{B} - \tfrac{1}{2}\mathbf{e}_x\,\frac{\partial}{\partial\xi}\,B^2,$$

we get

$$\sum_{\alpha\neq e}\frac{\rho_{0\alpha}U}{\Omega_\alpha}\mathbf{V}_\alpha - \tfrac{1}{2}\mathbf{e}_x\sum_a \beta_\alpha N_\alpha^{\gamma_\alpha} + B_x\mathbf{B} - \tfrac{1}{2}B^2\mathbf{e}_x = \text{const.} \tag{2.15}$$

Thereby we have introduced the unperturbed charge density $\rho_{0\alpha} = \kappa_\alpha Z_\alpha$. From the transverse components of (2.15), we can express the transverse proton velocities as

$$V_{py} = -\frac{\Omega_p\cos\theta}{\rho_{0p}U}\,B_y - \frac{\Omega_p}{\Omega_i}\,\frac{\rho_{0i}}{\rho_{0p}}\,V_{iy} \tag{2.16}$$

$$V_{pz} = -\frac{\Omega_p\cos\theta}{\rho_{0p}U}\,b_z - \frac{\Omega_p}{\Omega_i}\,\frac{\rho_{0i}}{\rho_{0p}}\,V_{iz}\ , \tag{2.17}$$

with $b_z = B_z - \sin\theta$. The longitudinal momentum component, see (2.15), as well as the total energy of the system, are conserved quantities, which are not used further in our analytical treatment. But they are used to check our subsequent numerical integration, since they must keep their constant values.

We now concentrate on the remaining differential equations. The longitudinal components of the momentum equations (2.3) and (2.4) can be written as

$$\frac{\partial}{\partial\xi}\,N_e = -\frac{N_e^3}{c_{se}^2 N_e^{\gamma_e+1}}\left(E_x - \frac{U\sin\theta}{\cos\theta}\,B_y\right), \tag{2.18}$$

$$\frac{\partial}{\partial\xi}\,N_p = \frac{\Omega_p N_p^3}{C_{sp}^2 N_p^{\gamma_p+1} - U^2}\left(E_x + V_{py}B_z - V_{pz}B_y\right), \tag{2.19}$$

$$\frac{\partial}{\partial\xi}\,N_i = \frac{\Omega_i N_i^3}{C_{si}^2 N_i^{\gamma_i+1} - U^2}\left(E_x + V_{iy}B_z - V_{iz}B_y\right), \tag{2.20}$$

with the abbreviations

$$c_{se}^2 = \tfrac{1}{2}\beta_e\gamma_e, \qquad C_{sp}^2 = \Omega_p\,\frac{\beta_p\gamma_p}{2\rho_{0p}}, \qquad C_{si}^2 = \Omega_i\,\frac{\beta_i\gamma_i}{2\rho_{0i}},$$

which are in intimate relationship to the plasma sound speeds. Owing to the

https://doi.org/10.1017/S0022377898007193 Published online by Cambridge University Press

quasineutrality (2.8), we get an expression for E_x from the three equations (2.18)–(2.20)

$$E_x = \left(\frac{N_e^3}{c_{se}^2 N_e^{\gamma_e+1}} + \frac{\rho_{0p}\mathbf{\Omega}_p N_p^3}{C_{sp}^2 N_p^{\gamma_p+1} - U^2} + \frac{\rho_{0i}\mathbf{\Omega}_i N_i^3}{C_{si}^2 N_i^{\gamma_i+1} - U^2} \right)^{-1} \times \left[\frac{N_e^3}{c_{se}^2 N_e^{\gamma_e+1}} \frac{U \sin\theta}{\cos\theta} B_y - \frac{\rho_{0p}\mathbf{\Omega}_p N_p^3}{C_{sp}^2 N_p^{\gamma_p+1} - U^2} \left(V_{py} B_z - V_{pz} B_y\right) - \frac{\rho_{0i}\mathbf{\Omega}_i N_i^3}{C_{si}^2 N_i^{\gamma_i+1} - U^2} \left(V_{iy} B_z - V_{iz} B_y\right) \right], \tag{2.21}$$

which can be used to eliminate E_x from the set of equations. After that, we need only two of them (the third can easily be constructed from (2.8)), and we drop (2.18) (which is somewhat arbitrarily chosen).

From the transverse components of (2.3), we need only the two equations for the transverse ion velocities,

$$\frac{\partial}{\partial\xi} V_{iy} = -\mathbf{\Omega}_i \left[b_z + \frac{\cos\theta}{U} N_i V_{iz} - \sin\theta \left(N_i - 1\right) \right], \tag{2.22}$$

$$\frac{\partial}{\partial\xi} V_{iz} = \mathbf{\Omega}_i \left(B_y + \frac{\cos\theta}{U} N_i V_{iy} \right), \tag{2.23}$$

and, from Ampèré's law (2.6), we get two equations for the magnetic field,

$$\frac{\partial}{\partial\xi} B_y = -\frac{N_p \mathbf{\Omega}_p \cos^2\theta - U^2}{U\cos\theta} b_z - \frac{\rho_{0i}}{\mathbf{\Omega}_i} \left(\mathbf{\Omega}_p N_p - \mathbf{\Omega}_i N_i\right) V_{iz} - \frac{U\sin\theta}{\cos\theta} \left(N_e - 1\right), \tag{2.24}$$

$$\frac{\partial}{\partial\xi} B_z = \frac{N_p \mathbf{\Omega}_p \cos^2\theta - U^2}{U\cos\theta} B_y + \frac{\rho_{0i}}{\mathbf{\Omega}_i} \left(\mathbf{\Omega}_p N_p - \mathbf{\Omega}_i N_i\right) V_{iy}. \tag{2.25}$$

We have ended up with a set of ordinary differential equations of order six in the variables N_p, N_i, V_{iy}, V_{iz}, B_y and B_z. All other variables that remain in the associated equations (2.19)–(2.20) and (2.22)–(2.25) can be expressed in terms of these six variables using the equations given above. Thus we may formally denote the system as

$$\frac{d}{d\xi}\mathbf{y} = \mathscr{F}(\mathbf{y}), \qquad \text{with} \quad \mathbf{y} = (N_p, N_i, V_{iy}, V_{iz}, B_y, B_z). \tag{2.26}$$

If we know appropriate initial values, we can easily integrate this system numerically (e.g. by a Runge–Kutta method), which is done in Sec. 4. But before we do so, we have to discuss the problems of initial values. This is necessary because the 'trivial' initial value $\mathbf{y}_0$, describing the unperturbed plasma, leads to $\mathscr{F}(\mathbf{y}_0) = 0$, which represents a fixed point and thus is not suitable as an initial value for our numerical integration.

3. Linearization at the fixed point

Since we are interested in solitary-wave solutions of the multifluid equations, we intend to search for necessary conditions for the existence of such solutions. A solitary wave represents a finite perturbation spatially localized in a special

https://doi.org/10.1017/S0022377898007193 Published online by Cambridge University Press

stationary frame of reference, i.e. the perturbation disappears at infinity. Thereby, the amplitude of the solitary wave decreases rapidly towards zero, i.e. the solution $\mathbf{y}$ approaches the fixed point $\mathbf{y}_0$. Since we can make the amplitude as small as we want by going farther and farther to the tail (respectively the fixed point), we should get an accurate description of the solitary wave's behaviour there, even if we use linearized equations.

Denoting by lower-case letters the very small disturbances from the fixed point, we obtain by linearization from (2.22)–(2.25)

$$\frac{\partial}{\partial\xi} v_{iy} = -\Omega_i\, b_z - \Omega_i \frac{\cos\theta}{U}\, v_{iz} + \Omega_i \sin\theta\, n_i \ , \tag{3.1}$$

$$\frac{\partial}{\partial\xi} v_{iz} = \Omega_i\, b_y + \Omega_i \frac{\cos\theta}{U}\, v_{iy} \ , \tag{3.2}$$

$$\frac{\partial}{\partial\xi} b_y = -\frac{\Omega_p \cos^2\theta - U^2}{U\cos\theta}\, b_z - \rho_{0i} \frac{\Omega_p - \Omega_i}{\Omega_i}\, v_{iz} - \frac{U\sin\theta}{\cos\theta}\, n_e \ , \tag{3.3}$$

$$\frac{\partial}{\partial\xi} b_z = \frac{\Omega_p \cos^2\theta - U^2}{U\cos\theta}\, b_y + \rho_{0i} \frac{\Omega_p - \Omega_i}{\Omega_i}\, v_{iy} \ . \tag{3.4}$$

This set of equations is closed if we know $n_i(v_{iy}, v_{iz}, b_y, b_z)$ and $n_e(v_{iy}, v_{iz}, b_y, b_z)$. We shall deduce these two functions now (which is possible in the case of linearized equations). From (2.20) and (2.21), we get

$$\frac{\partial}{\partial\xi} n_i = -\frac{\Omega_i \sin\theta}{(U^2 - C_{s1}^2)(U^2 - C_{s2}^2)} \left\{ \frac{1}{U\cos\theta} (U^4 - C_{sp}^2 U^2 - \Omega_p c_{se}^2 \cos^2\theta)\, b_y \right. \\ \left. + \left[U^2 - C_{sp}^2 - \frac{\Omega_p}{\Omega_i} (\Omega_p \rho_{0i} + \Omega_i \rho_{0p}) c_{se}^2 \right] v_{iy} \right\}, \tag{3.5}$$

with

$$(U^2 - C_{s1}^2)(U^2 - C_{s2}^2) = U^4 - U^2 \left[C_{sp}^2 + C_{si}^2 + (\Omega_p \rho_{0p} + \Omega_i \rho_{0i})\, c_{se}^2 \right] \\ + C_{sp}^2 C_{si}^2 + (\Omega_p \rho_{0p} C_{si}^2 + \Omega_i \rho_{0i} C_{sp}^2)\, c_{se}^2 \ . \tag{3.6}$$

C_{s1} and C_{s2} are the sound speeds of the plasma (Mann *et al.* 1997). Note that all three equations (3.2), (3.4), and (3.5) depend linearly on b_y and v_{iy}. Therefore a linear combination of them exists where the left-hand side is a differential and the right-hand side vanishes. Integration of this differential yields

$$n_i = \frac{\Omega_i \sin\theta}{(U^2 - C_{s1}^2)(U^2 - C_{s2}^2)} \left[\Omega_p c_{se}^2\, b_z - \frac{U}{\Omega_i \cos\theta} (U^2 - C_{sp}^2 - \Omega_p c_{se}^2)\, v_{iz} \right] , \tag{3.7}$$

which is the first function we have been looking for. Then the second function is straightforwardly obtained from the linearized longitudinal component of (2.15) by inserting (3.7) and taking (2.8) into account:

$$n_e = \frac{\sin\theta}{(U^2 - C_{s1}^2)(U^2 - C_{s2}^2)} \left\{ \Omega_p (U^2 - C_{si}^2)\, b_z \right. \\ \left. + \frac{\rho_{0i} U}{\Omega_i \cos\theta} [\Omega_p (U^2 - C_{si}^2) - \Omega_i (U^2 - C_{sp}^2)]\, v_{iz} \right\}. \tag{3.8}$$

We can now discuss the kind of solutions that our linearized set of equations

https://doi.org/10.1017/S0022377898007193 Published online by Cambridge University Press

(3.1)–(3.4) possess, denoted by

$$\frac{d}{d\xi}\,\mathbf{y}_l = \mathscr{A}\mathbf{y}_l, \qquad \text{i.e.} \quad \frac{d}{d\xi}\begin{pmatrix} b_y \\ b_z \\ v_{iy} \\ v_{iz} \end{pmatrix} = \begin{pmatrix} 0 & a_1 & 0 & a_2 \\ a_3 & 0 & a_4 & 0 \\ 0 & a_5 & 0 & a_6 \\ a_7 & 0 & a_8 & 0 \end{pmatrix}\begin{pmatrix} b_y \\ b_z \\ v_{iy} \\ v_{iz} \end{pmatrix}. \tag{3.9}$$

The characteristic polynomial of the constant matrix $\mathscr{A}$,

$$\chi_{\mathscr{A}}(\lambda) = \det(\mathscr{A} - \lambda\mathbf{1}) = \lambda^4 + p\lambda^2 + q, \tag{3.10}$$

is biquadratic with coefficients

$$p = -(a_1a_3 + a_2a_7 + a_4a_5 + a_6a_8), \qquad q = (a_1a_6 - a_2a_5)(a_3a_8 - a_4a_7),$$

owing to the 'symmetric' distribution of zeros in $\mathscr{A}$. We get four eigenvalues $\lambda_1, \ldots, \lambda_4$, which are the roots of the characteristic polynomial (3.10). We shall not concentrate on the case of multiple eigenvalues. The general solution of (3.9) is

$$\mathbf{y}_l(\xi) = c_1\hat{\mathbf{y}}_1\, e^{\lambda_1\xi} + c_2\hat{\mathbf{y}}_2\, e^{\lambda_2\xi} + c_3\hat{\mathbf{y}}_3\, e^{\lambda_3\xi} + c_4\hat{\mathbf{y}}_4\, e^{\lambda_4\xi}, \tag{3.11}$$

where the c_ν (with $\nu = 1, \ldots, 4$) and the $\hat{\mathbf{y}}_\nu$ denote arbitrary complex numbers and the (normalized) eigenvectors associated with λ_ν respectively. Since $a_1, \ldots, a_8$ are real numbers, it is always possible to construct a real solution $\mathbf{y}_l(\xi)$ by choosing appropriate c_ν.

Since the solitary wave approaches the fixed point at infinity, there must be a regime in our solution $\mathbf{y}_l(\xi)$ growing (or diminishing) exponentially with ξ. Otherwise, if there were oscillation with a constant amplitude, i.e. all lambdas were purely imaginary, the solution would always stay at the same (very small) amplitude. Thus we have found a necessary condition for the existence of solitary waves: at least one of the lambdas must have a non-vanishing real part (owing to the biquadratic structure of (3.10), there is always a second lambda with the opposite sign).

For an exhaustive analysis of the 'regions of possible soliton existence', it is a good idea to look at the boundaries of these regions. Since the regions are characterized by $p^2 \geqslant 4q$ and $\lambda^2 > 0$ as well as by $p^2 < 4q$, we have to look for $\lambda = 0$ (respectively $q = 0$) ($p^2 \geqslant 4q$ is then fulfilled as well) or to look for $p^2 = 4q$. Also, at a pole λ^2 may change its sign: the poles are located at $U = C_{s1}$ and $U = C_{s2}$. If we know the boundaries, we have to check the lambdas at just one point inside each bordered region.

In Fig. 1 we show the results of the aforementioned analysis for a helium–proton–electron plasma with 10 % helium ions, i.e. $\kappa = 0.1$, $M = 4$ and $Z = 2$. The plasma is slightly warm (the particle temperatures $T_e = 4T_p = 4T_i$; more specifically, $\beta_e = 0.4$, $\beta_p = 0.08$ and $\beta_i = 0.01$). Thus the only remaining free parameters are the velocity U of the solitary wave and the propagation angle θ with respect to the ambient magnetic field. In the light- and dark-shaded regions of Fig. 1 solitons may exist, whereas in the white regions only purely oscillatory solutions can be found. The solid lines mark boundaries with $\lambda = 0$, and the dashed lines indicate the two poles at $U = C_{s1}$ and $U = C_{s2}$. The dotted lines enclose regions with $p^2 < 4q$, where all four lambdas are complex numbers. Apart from in these latter regions, the lambdas are either real or purely imaginary. In the light-shaded regions two of the lambdas are real; in the dark-shaded regions all four of them are real.

Since we have solved the linear equations, we can easily calculate an appropriate initial value for the nonlinear problem: we take our linear solution and scale it

https://doi.org/10.1017/S0022377898007193 Published online by Cambridge University Press

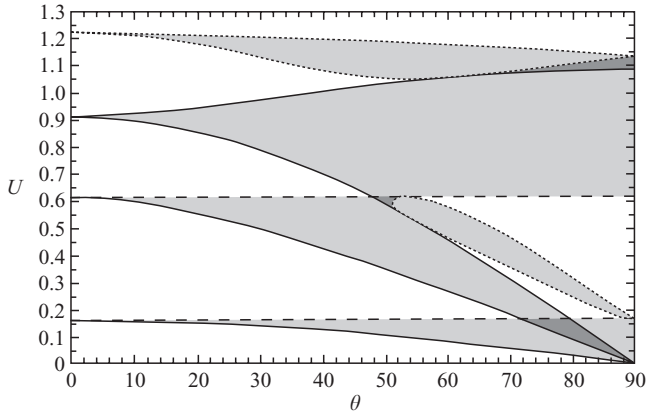


Figure 1. Possible regions of existence (grey-shaded) for solitary waves, depending on the propagation speed U and the angle of propagation θ with respect to the ambient magnetic field. For a detailed description of this figure and the plasma parameters, see the text.

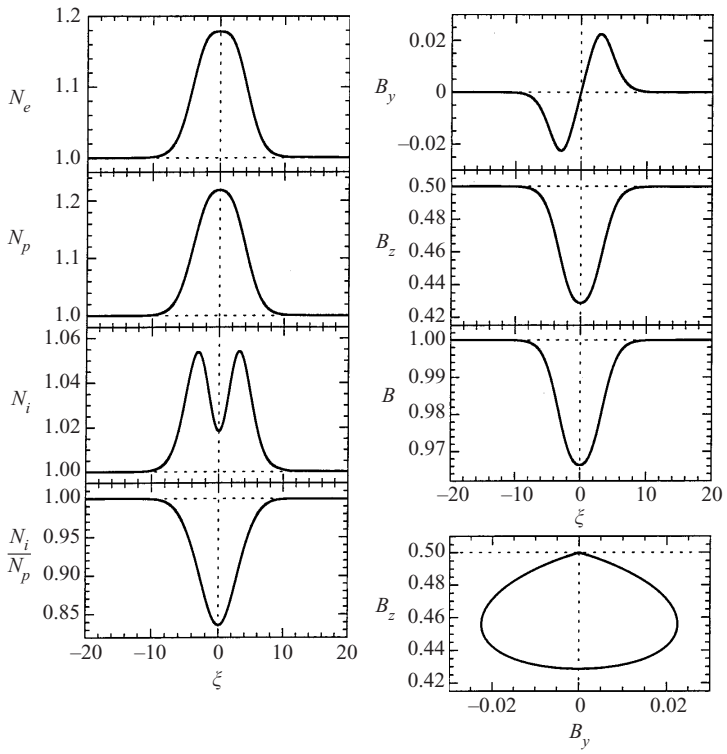


Figure 2. Solitary-wave solution for $U = 0.55$ and $\theta = 30°$. The plasma properties are described in the text at the end of Sec. 3. The left-hand panels show the normalized particle densities of the electrons, protons and helium ions versus the normalized spacial coordinate, which is centred on the maximum of the solitary wave. The bottom panel shows the relative abundance of helium ions with respect to the protons. On the right-hand side the magnetic field is depicted. The x component is not shown, since it is constant at $B_x = \cos\theta$. The bottom panel shows a hodogram, i.e. B_z as a function of B_y.

https://doi.org/10.1017/S0022377898007193 Published online by Cambridge University Press

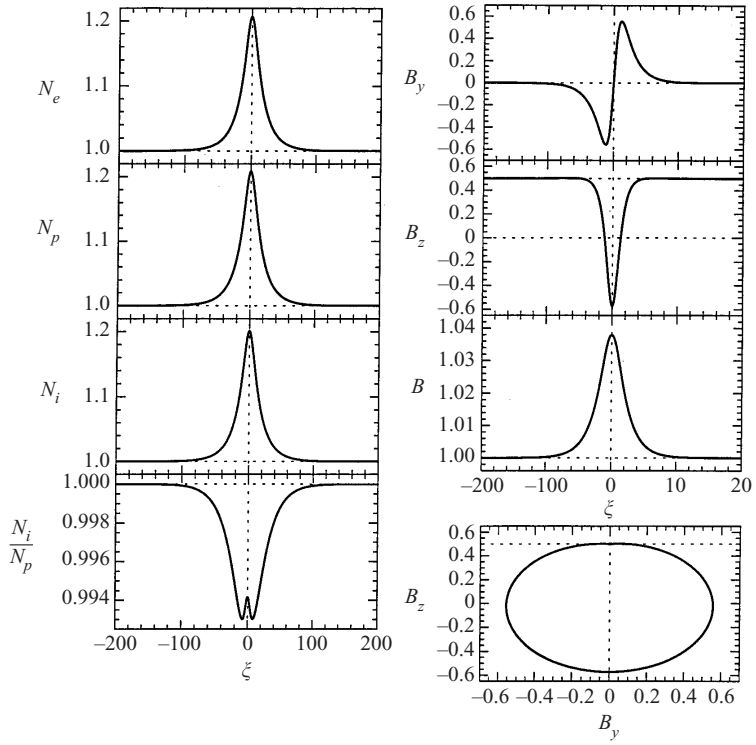


Figure 3. Solitary-wave solution for $U = 0.793$ and $\theta = 30°$. See Fig. 2 for details.

down to a sensibly small perturbation (typically $|\mathbf{y}_l| \approx 10^{-8}, \ldots, 10^{-5}$). Then we calculate the particle densities n_p and n_i by means of (2.8), (3.7) and (3.8), and add the perturbation to the unperturbed plasma values $\mathbf{y}_0$. With this initial value, we start a numerical integration of (2.26).

4. Solitary waves

With (2.26), we have developed our set of ordinary differential equations, and in the last section we have discussed a method to get an appropriate initial value for the integration of these equations. We numerically integrate them by applying a fifth-order Runge–Kutta method (cf. the routines *rkqs* and *rkck* in Press *et al.* 1992).

Since the 'regions of possible soliton existence' (see Fig. 1) do not guarantee the actual existence of a solitary wave, we have to check this by carrying out the numerical integration. If we are successful in finding a soliton, our solution $\mathbf{y}(\xi)$, which begins at the initial value $\mathbf{y}_i$, must first rise, then drop and finally approach the fixed point $\mathbf{y}_0$ again. If we come as close to the fixed point as our initial value, i.e. $|\mathbf{y}(\xi) - \mathbf{y}_0| < |\mathbf{y}_i - \mathbf{y}_0|$, we can stop the numerical integration and conclude that we have indeed found a solitary-wave solution (see Figs 2–6).

But it is also possible that we run into one of the poles of (2.19) and (2.20). Then the particle number density has a vertical tangent, and subsequently the solution takes imaginary values. A further integration is not sensible, and we must discard such a solution.

Note that we have to try two different initial values $\mathbf{y}_{i1,2}$ for each linear solution

https://doi.org/10.1017/S0022377898007193 Published online by Cambridge University Press

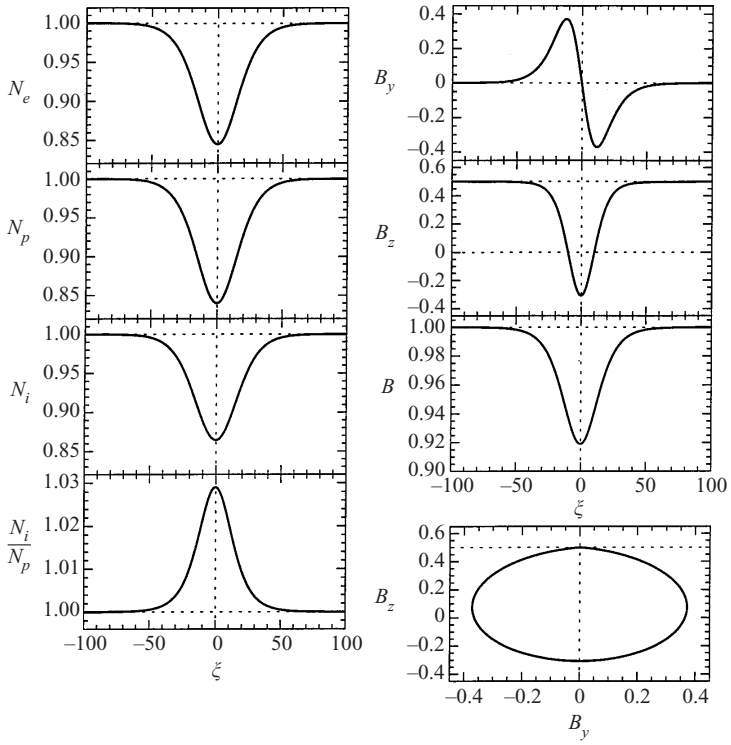


Figure 4. Solitary-wave solution for $U = 0.8$ and $\theta = 30°$. See Fig. 2 for details.

$\mathbf{y}_l$, because if $\mathbf{y}_l$ is a solution of (3.9) then so also is $-\mathbf{y}_l$. Owing to the above-mentioned poles, we usually find a solution only for one initial value. But it is also possible to find two different solutions (see Figs 5 and 6) for the same set of parameters (because of the two different initial values). It may also happen that for some parameters there is no solution at all.

We have carried out the above integrations at several exemplary points of the (U, θ) plane (see Fig. 1). The results are given in Figs 2–6, where we show the normalized particle number densities and the magnetic field. Additionally, we have compared the proton number density with the ion number density by means of the ratio N_p/N_i. If there is a mere plasma compression within the solitary wave than this quotient keeps very close to the value 1, which is approximately fulfilled in Figs 3 and 4. Furthermore, we have displayed magnetic field hodograms, i.e. the variation of B_z with respect to B_y.

The propagation speed U of the solitary wave shown in Fig. 2 lies between the two sound speeds C_{s1} and C_{s2}. It is comparable to the solitary wave shown in Fig. 5, where speed is also located between the two sound speeds, but in contrast to that wave it shows a distinct proton enrichment ($N_i/N_p < 1$). The helium ions are only slightly enriched, with a drop in the middle of the solitary wave.

The two solitary waves shown in Figs 3 and 6 show an increase in the magnetic field strength B. We could observe this phenomenon only for solitary waves with speeds $U \approx v_A \cos\theta$ in the vicinity of the Alfvén speed times the cosine of the propagation angle, i.e. the phase speed of transversely propagating Alfvén waves.

We can distinguish another two types of solitary waves: fast solitary waves with

https://doi.org/10.1017/S0022377898007193 Published online by Cambridge University Press

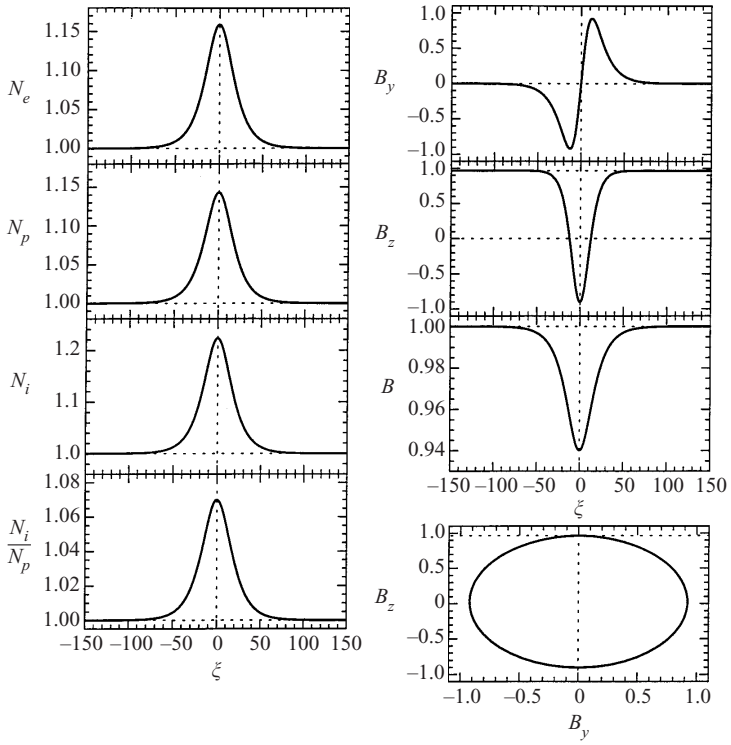


Figure 5. Solitary-wave solution for $U = 0.236$ and $\theta = 75°$. See Fig. 2 for details.

$U > C_{s1}, C_{s2}$ and slow solitary waves with $U < \max(C_{s1}, C_{s2})$. For fast waves (Figs 3 and 4) the electron density is correlated with the magnetic field strength, whereas for slow waves they are anticorrelated (Figs 2, 5 and 6). This fact is also well known from slow and fast MHD waves (see e.g. Krall and Trivelpiece 1973).

5. Final remarks

To the best of our knowledge, this is the first time that solitary waves, which are based on the full nonlinear equations, have been found theoretically in a multi-ion plasma.

We began our calculations with fluid equations applied to a homogeneous three-component plasma. These equations have been simplified by the assumption of one-dimensional propagation and stationarity in a comoving frame of reference. Thus the partial differential equations have been reduced to a set of ordinary differential equations (ODEs) of order six (see (2.26)).

The unperturbed plasma is a fixed point of these ODEs. The solitary wave of our interest tends towards this fixed point if we move away from the crest to the edges of the solitary wave, where we obtain very small amplitudes and therefore must have a close look at the linearized equations. In this analysis two things have been found: a necessary condition for the existence of solitary waves (see Fig. 1) and suitable initial values for the beginning of the numerical integration of our ODEs.

We have performed the numerical integration at a few chosen parameters and

https://doi.org/10.1017/S0022377898007193 Published online by Cambridge University Press

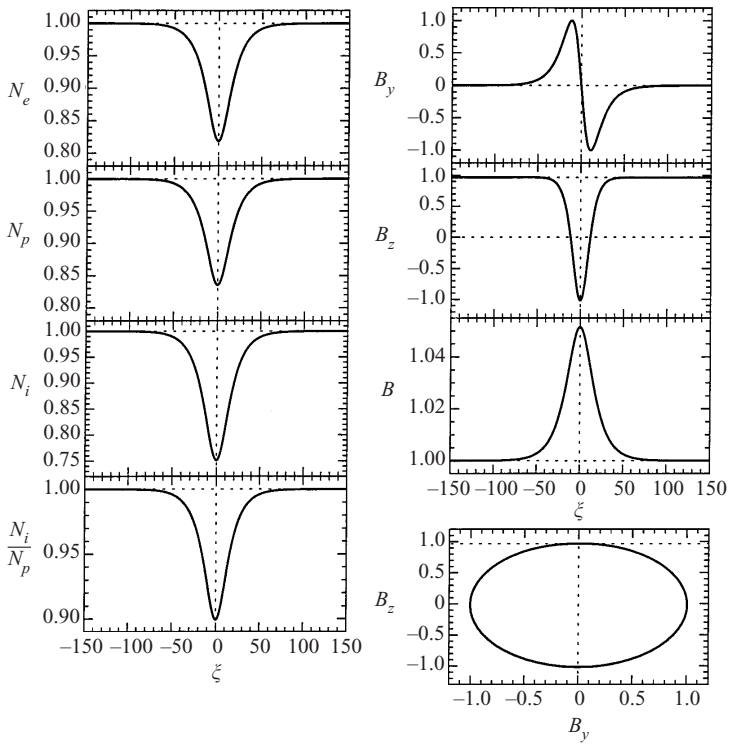


Figure 6. Solitary-wave solution for $U = 0.236$ and $\theta = 75°$. See Fig. 2 for details.

have presented the solitary waves found thereby. Solitary waves with increasing and decreasing magnetic field strength have been found. Also a correlation (anti-correlation) between magnetic field and particle number density for fast (slow) solitary waves could be observed, as for fast (slow) waves in pure MHD.

Furthermore, the abundance of ions within the wave is not fixed, but varies spatially, and an enrichment or depletion of one species with respect to the other is found. This goes beyond the effects observed with the pure compression of a plasma.

It needs to be proved whether or not the solitary waves are stable. Also, in situ measurements (spacecraft data) should be compared with our numerical results. However, one should bear in mind that for this purpose high-time-resolution data are necessary: if we assume that the solar wind (500 km s^{-1}) sweeps the solitary wave over the (nearly resting) spacecraft, and the typical dimension of the wave is about 10–100 ion inertial lengths (which results in about 1000–10 000 km under typical solar wind conditions), then the whole transit of the wave happens within 2–20 s. For a comparison, we need at least eight sample points, containing the magnetic field information *and* the particle densities (both the proton and the helium densities). Thus the required time resolution is better than 0.25–2.5 s, which is rather fast for today's particle measurements.

It should be noted that the method for deriving (2.26) is not confined to solitary waves only. By merely taking other integration constants (due to other boundary conditions), a very similar set of ODEs can be derived that is appropriate for the description of nonlinear waves.

https://doi.org/10.1017/S0022377898007193 Published online by Cambridge University Press

Acknowledgements

We are indebted to K. Baumgärtel for useful discussions. We thank the Deutsche Forschungsgemeinschaft for supporting this work under Grants Ma 1376/6-1 and 1376/6-2.

References

Baumgärtel, K., Dubinin, E., Sauer, K. and Story, T. R. 1997 Solar wind magnetic holes: signatures of slow-mode type MHD solitons? *Adv. Space Res.* **20**, 69–74.

Bird, K. M. and Edenhofer, P. 1990 Remote sensing observations of the solar corona. *Physics of the Inner Heliosphere I: Large-Scale Phenomena* (ed. R. Schwenn and E. Marsch), pp. 13–97. Vol. 20 of *Physics and Chemistry in Space*. Springer-Verlag, Berlin.

Fairfield, D. H. and Behannon, K. W. 1976 Bow shock and magnetosheath waves at Mercury. *J. Geophys. Res.* **81**, 3897–3906.

Gnavi, G., Gomberoff, L., Gratton, F. T. and Galvão, R. M. O. 1996 Electromagnetic ion-beam instabilities in a cold plasma. *J. Plasma Phys.* **55**, 77–86.

Goldstein, M. L., Smith, C. W. and Matthaeus, W. H. 1983 Large amplitude MHD waves upstream of the Jovian bow shock. *J. Geophys. Res.* **88**, 9989–9999.

Hoppe, M. M., Russell, C. T., Frank, L. A., Eastman, T. E. and Greenstadt, E. W. 1981 Upstream hydromagnetic waves and their association with backstreaming ion populations: Isee 1 and 2 observations. *J. Geophys. Res.* **86**, 4471–4492.

Isenberg, P. A. and Hollweg, J. V. 1982 Finite amplitude Alfvén waves in a multi-ion plasma: propagation, acceleration, and heating. *J. Geophys. Res.* **87**, 5023–5029.

Kakutani, T., Kawahara, T. and Taniuti, T. 1967 Nonlinear hydromagnetic solitary waves in a collision-free plasma with isothermal electron pressure. *J. Phys. Soc. Japan* **23**, 1138–1149.

Krall, N. A. and Trivelpiece, A. W. 1973 *Principles of Plasma Physics*. McGraw-Hill, New York (reprinted 1986 San Francisco Press).

McKenzie, J. F., Marsch, E., Baumgärtel, K. and Sauer, K. 1993 Wave and stability properties of multi-ion plasmas with applications to winds and flows. *Ann. Geophys.* **11**, 341–353.

Mann, G. and Lühr, H. 1991 Comparison of low frequency magnetic field fluctuations upstream of Earth's bow shock with a strong Alfvénic turbulence model. *Ann. Geophys.* **9**, 681–689.

Mann, G., Hackenberg, P. and Marsch, E. 1997 Linear mode analysis in multi-ion plasmas. *J. Plasma Phys.* **58**, 205–221.

Mariani, F. and Neubauer, F. M. 1990 The interplanetary magnetic field. *Physics of the Inner Heliosphere I: Large-Scale Phenomena* (ed. R. Schwenn and E. Marsch), pp. 183–206. Vol. 20 of *Physics and Chemistry in Space*. Springer-Verlag. Berlin.

Marsch, E., Mühlhäuser, K.-H., Rosenbauer, H., Schwenn, R. and Neubauer, F. M. 1982 Solar wind helium ions: observations of the Helios solar probes between 0.3 and 1 AU. *Geophys. Res. Lett.* **87**, 35–51.

Miller, J. A. and Viñas, A. F. 1993 Ion acceleration and abundance enhancements by electron beam instabilities in impulsive solar flares. *Astrophys. J.* **412**, 386–400.

Oscarson, T. and André, M. 1986 Waves with frequencies below the proton gyrofrequency in a multicomponent plasma. *Ann. Geophys.* **4**, 319–325.

Paschmann, G., Sckopke, N., Bame, S. J., Asbridge, J. R., Gosling, J. T., Russell, C. T. and Greenstadt, E. W. 1979 Association of low-frequency waves with suprathermal ions in the upstream solar wind. *Geophys. Res. Lett.* **6**, 209–212.

Press, W. H., Teukolsky, S. A., Vetterling, W. T. and Flannery, B. P. 1992 *Numerical Recipes in Fortran: The Art of Scientific Computing*. Cambridge University Press.

Thompson, P., Dougherty, M. K. and Southwood, D. J. 1995 Wave behaviour near critical frequencies in cold bi-ion plasmas. *Planet. Space Sci.* **43**, 625–634.

Tsurutani, B. T. 1991 Cometary plasma waves and instabilities. *Comets in the Post-Halley Era*, Vol. 2 (ed. R. L. Newburn, Jr *et al.*, pp. 1171–1210. Kluwer, Dordrecht.

https://doi.org/10.1017/S0022377898007193 Published online by Cambridge University Press

Tsurutani, B. T., Ho, C. M., Arballo, J. K. and Goldstein, B. E. 1995 Large amplitude IMF fluctuations in corotating interaction regions: Ulysses at midlatitude. *Geophys. Res. Lett.* **22**, 3397–3400.

Turner, J. M., Burlaga, L. F., Ness, N. F. and Lemaire, J. F. 1977 Magnetic holes in the solar wind. *J. Geophys. Res.* **82**, 1921–1924.

Verheest, F. 1990 Nonlinear parallel Alfvén waves in cometary plasmas. *Icarus* **86**, 273–282.

Winterhalter, D., Neugebauer, M., Goldstein, B. E., Smith, E. J., Bame, S. J. and Balogh, A. 1994 Ulysses field and plasma observations of magnetic holes in the solar wind and their relation to mirror-mode structures. *J. Geophys. Res.* **99**, 23 371–23 381.

https://doi.org/10.1017/S0022377898007193 Published online by Cambridge University Press